AAPT PHYSICS EDUCATION | AMERICAN JOURNAL of PHYSICS

A demonstration of the conservation of the orbital angular momentum of Earth

Leonardo J. Pellizza, Mariano G. Mayochi, Ligia Ciocci Brazzano, and Susana E. Pedrosa

Citation: American Journal of Physics **83**, 1019 (2015); doi: 10.1119/1.4932397
View online: http://dx.doi.org/10.1119/1.4932397
View Table of Contents: http://scitation.aip.org/content/aapt/journal/ajp/83/12?ver=pdfcov
Published by the American Association of Physics Teachers

A demonstration of the conservation of the orbital angular momentum of Earth

Leonardo J. Pellizza[a),b)]
Instituto Argentino de Radioastronomía (CONICET), C.C. 5, B1894ZAA, Villa Elisa, Pcia. de Buenos Aires, Argentina

Mariano G. Mayochi
Scuola Italiana Cristoforo Colombo, Ramsay 2251, C1428BAI, Buenos Aires, Argentina and Dpto. de Física "J.J. Giambiagi," FCEyN, Universidad de Buenos Aires, Int. Güiraldes 2620, C1428EGA, Buenos Aires, Argentina

Ligia Ciocci Brazzano
Facultad de Ingeniería, Universidad de Buenos Aires, Av. Paseo Colón 850, C1063ACV, Buenos Aires, Argentina

Susana E. Pedrosa[b)]
Instituto de Astronomía y Física del Espacio (CONICET/UBA), C.C. 67, Suc. 28, C1428ZAA, Buenos Aires, Argentina

(Received 27 December 2014; accepted 21 September 2015)

We describe a simple but quantitative experiment to demonstrate the conservation of angular momentum. We measure the correlation of the apparent radius and angular velocity of the Sun with respect to the stars, due to the conservation of the angular momentum of Earth in its orbit. We also determine the direction of Earth's angular momentum vector and show that it is conserved. The experiment can be performed using a small telescope and a digital camera. It is conceptually simple, allowing students to get direct physical insight from the data. The observations are performed near the resolution limit imposed by the atmosphere, and in the presence of strong competing effects. These effects necessitate a careful experimental setup and allow students to improve their skills in experimentation.
[http://dx.doi.org/10.1119/1.4932397]

I. INTRODUCTION

The principle of conservation of angular momentum is a pillar of physics, playing a fundamental role in classical mechanics, electromagnetism, and quantum mechanics.[1–3] In spite of its importance, in most courses the conservation of angular momentum is approached from a theoretical point of view. The experiments usually used to demonstrate it in the classroom are merely qualitative in nature.[4–11] Indeed, a literature search reveals only a few student experiments in which this conservation law is tested quantitatively.[12–16]

Because gravity is a central force, the angular momentum of Earth is conserved in its orbital motion around the Sun. This simple system provides then a laboratory to obtain direct evidence supporting both the aforementioned conservation principle and the central nature of one of the fundamental interactions. Hence, a demonstration of the conservation of the orbital angular momentum of our planet can be a valuable experiment for undergraduate students. Moreover, the simplicity of the system allows a direct and clear interpretation of the data, increasing the value of the experiment as a teaching tool. The direction and distance to the Sun can be estimated from the position of the solar disk in the sky and its apparent size, respectively. The transverse velocity of Earth can be obtained from the apparent motion of the Sun with respect to the stars, while the radial velocity component is not needed, as it cancels in the vector product defining the angular momentum.

The feasibility, and also the difficulty, of this experiment can be understood by examining the amount of change of the observables to be measured, i.e., the solar apparent size and velocity. In fact, what one would measure is the angular velocity of Earth in its orbit, which multiplied by the square of the distance to the Sun gives the angular momentum per unit mass. The amplitude of the fractional variation of the distance between the Sun and Earth is given by twice the eccentricity of Earth's orbit ($e_\oplus = 0.017$), so it is roughly 3.4%. Given that the apparent diameter of the solar disk is ∼32 arc min, its maximum variation during the year would be of the order of 1 arc min. An angular resolution at least an order of magnitude better than this value (i.e., ∼6 arc sec, or 0.3% of the disk size) is needed to track this variation during the year. This value approaches the resolution limit imposed by Earth's atmosphere, providing an important challenge to the experimentalist. The expected variation of Earth's angular velocity is twice that of the distance, or ∼7%, because angular momentum is conserved. An order-of-magnitude estimate of the angular velocity of Earth is 1° day^{-1} (as it moves 360° in a sidereal year), therefore, the amplitude of its variation is ∼4 arc min day^{-1}. Observing the variation during the whole year requires therefore a resolution an order of magnitude better than this figure, or ∼20 arc sec day^{-1}. If the angular velocity is derived from the change of the position of the Sun over two consecutive days, a resolution of a few arcsec is enough for the purpose. The challenge here is to separate this effect from the far greater effect of the diurnal apparent motion of the Sun, produced by Earth's rotation. The latter is greater than the former by a factor of ∼366, equal to the ratio of one sidereal year to one sidereal day, as the angular velocity of Earth's rotation is 360° per sidereal day.

In this paper, we present an experiment designed to demonstrate the conservation of the orbital angular momentum

of Earth. We perform our experiment using a digital camera and a small telescope. The choice of these devices is dictated by the fact that present-day cameras with megapixel sensors can image the entire solar disk while discriminating variations of less than 0.1% of its diameter. Hence, they are able to reach the resolution needed for the experiment. Apart from the benefits described above, this experiment offers an opportunity to train undergraduate students in astronomical observing techniques, in which the experimental conditions cannot be completely controlled, requiring careful planning, setup, and execution of the experiment. At the same time, because the Sun is observable almost every day from many places in the world and is the brightest object in the sky, the proposed experiment is easy to fit into most course schedules.

The organization of this paper is as follows. Section II gives the theoretical framework of the experiment; Sec. III shows our experimental setup and procedure; and Sec. IV our data analysis. Finally, Sec. V presents our conclusions.

II. THEORY

Earth moves under the influence of the gravitational forces of all bodies in the Solar System. The Sun, with a mass $M_\odot = 1.99 \times 10^{30}$ kg and at a mean distance $\bar{r}_\odot = 1.46 \times 10^{11}$ m, exerts by far the greatest gravitational force on Earth, so we will neglect the influence of all other bodies and consider only the Earth-Sun system. Because the mass of Earth is $M_\oplus = 5.97 \times 10^{24}$ kg $\ll M_\odot$, the Sun can be considered a fixed center of force, around which Earth revolves in a plane (i.e., the plane of the ecliptic), within which it describes an elliptical orbit. The energy and angular momentum of Earth are conserved, because the gravitational force is both conservative and central.

In the following discussion, we will assume that we can define an inertial reference frame fixed to the stars. We will also neglect the motion of the Sun with respect to this inertial frame, so the reference frame fixed to the Sun is also inertial. Both assumptions are justified because the motion of Earth around the Sun involves length and time scales much smaller than those involved in the relative motions of the stars.

The angular momentum of Earth with respect to the Sun (Fig. 1, left panel) is

$$\vec{L}_\oplus = M_\oplus \vec{r}_\oplus \times \vec{v}_\oplus = M_\oplus \vec{r}_\odot \times \vec{v}_\odot, \tag{1}$$

where $\vec{r}_\oplus$ and $\vec{v}_\oplus$ are the position and velocity of Earth in a reference frame fixed to the Sun, respectively. The position and velocity of the Sun observed from Earth are $\vec{r}_\odot = -\vec{r}_\oplus$ and $\vec{v}_\odot = -\vec{v}_\oplus$. The magnitude of $\vec{L}_\oplus$ is

$$L_\oplus = M_\oplus r_\odot v_{\mathrm{t},\odot} = M_\oplus \omega r_\odot^2, \tag{2}$$

where $v_{\mathrm{t},\odot}$ is the component of $\vec{v}_\odot$ normal to $\vec{r}_\odot$, and $\omega = v_{\mathrm{t},\odot} r_\odot^{-1}$ is the angular velocity of the Sun with respect to the stars as seen from Earth. The instantaneous distance of the Sun $r_\odot$ can be determined from its physical radius $R_\odot = 6.96 \times 10^8$ m and the apparent radius of the solar disk $\phi_\odot$, as

$$r_\odot = R_\odot \phi_\odot^{-1}, \tag{3}$$

where we have used $\phi_\odot \ll 1$. Combining Eqs. (2) and (3), we get

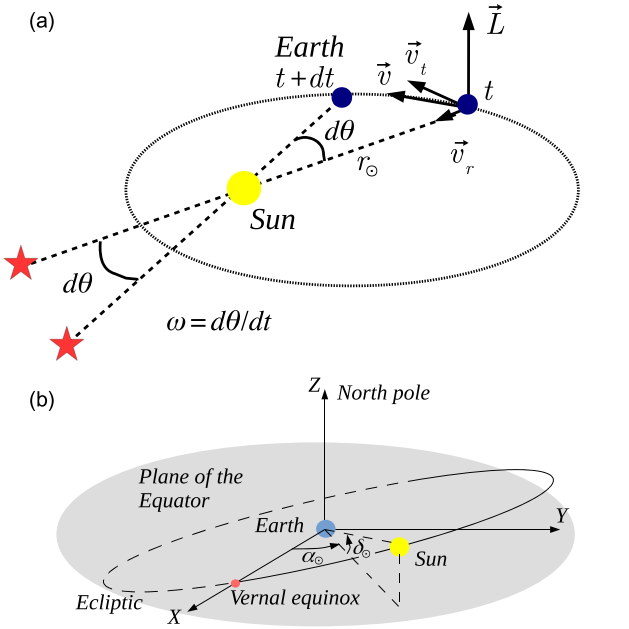

Fig. 1. Upper panel: The orbit of Earth around the Sun, as seen from an inertial frame fixed to the stars. The angular momentum $\vec{L}$ and velocity $\vec{v}$ are shown, together with the decomposition of the latter in the radial and transverse directions. The Sun is at an instantaneous distance $r_\odot$ from Earth. Dashed lines represent the line of sight to the Sun from Earth at times t and $t+dt$, and show that the angle $d\theta$ swept by our planet in the interval dt is the same as the observed change in the position of the Sun with respect to the stars. Therefore, the rate of this change is equal to the angular velocity of Earth. Lower panel: The equatorial reference frame fixed to Earth. The shaded region is the equatorial plane, and the ellipse represents the ecliptic. Their intersection is the direction of the vernal equinox, toward which the X-axis points. The rotation axis of Earth is the Z-axis; the Y-axis is defined by the right-handedness of the frame. Right ascension α and declination δ are the spherical angular coordinates of this frame.

$$\omega = L_\oplus M_\oplus^{-1} R_\odot^{-2} \phi_\odot^2. \tag{4}$$

This equation has the advantage of being written in terms of observables; hence, it can be used to demonstrate the conservation of $L_\oplus$. A series of simultaneous measurements of $\phi_\odot$ and ω should show a correlation, in the sense that ω increases with $\phi_\odot$. The existence of the correlation described by Eq. (4) would provide a direct piece of evidence for the conservation of the magnitude of Earth's angular momentum $L_\oplus$. The constancy of the direction of the angular momentum $\hat{L}_\oplus$ can be demonstrated by measuring the directions $\hat{r}_\odot$ and $\hat{v}_{\mathrm{t},\odot}$, and showing that their vector product is constant. The radial component of the velocity of the Sun with respect to Earth cancels out in the vector product, so it does not need to be measured.

However, some care must be taken to determine ω because observers on Earth's surface are fixed to a rotating reference frame. The actual angular velocity of the Sun in the sky is the composition of the apparent motion of the Sun with respect to the stars, due to the orbital motion of Earth, plus the diurnal motion of all celestial bodies, due to the rotation of our planet (i.e., the angular velocity of the rotating frame). In order to measure ω, the effect of Earth's rotation must be corrected for. The easiest way to do this is to measure the change in the position of the Sun in the equatorial astronomical reference frame (Fig. 1, right panel).[17] This is the closest realization of a non-rotating frame fixed to Earth; its axes (X, Y, Z) are defined by the direction of Earth rotation axis (Z, with its unit

vector $\hat{Z}$ pointing North), and the direction of the intersection of the orbital and equatorial planes of Earth (X, $\hat{X}$ pointing in the direction of the vernal equinox). The Y-axis is orthogonal to X and Z, and $\hat{Y}$ is defined by the fact that the system is right-handed. Within this frame, the spherical angular coordinates *right ascension* (α) and *declination* (δ) are used. The former is the usual azimuthal angle of any spherical system, while the latter is the complement of the polar angle. The equatorial coordinates of the Sun ($\alpha_\odot$, $\delta_\odot$) change only due to the motion of our planet in its orbit. We disregard here other small, long-term variations of equatorial coordinates due to the change in the orientation of the rotation axis of our planet, such as precession or nutation,[17] which are negligible for our purposes.

The equatorial coordinates of the Sun can be related to observables if we consider its position at transit, i.e., at the time the center of the solar disk crosses the meridian of the observer.[18] First,

$$\delta_\odot = \varphi \pm z_\odot^{\mathrm{t}}, \tag{5}$$

where $z_\odot^{\mathrm{t}}$ is the Sun zenith distance at transit, φ is the latitude of the observer, and the plus (minus) sign applies when the transit occurs to the north (south) of the zenith. Second,

$$\alpha_\odot - \alpha_\star = \Omega_\oplus (t_\odot^{\mathrm{t}} - t_\star^{\mathrm{t}}) \,|\, 2\pi, \tag{6}$$

where $t_\odot^{\mathrm{t}}$ and $t_\star^{\mathrm{t}}$ are the transit times of the Sun and a star with right ascension $\alpha_\star$, respectively, $\Omega_\oplus = 7.29 \times 10^{-5}$ s^{-1} is the sidereal rotational angular velocity of Earth, and $|$ represents the modulo operation.[19] Both $z_\odot^{\mathrm{t}}$ and the transit times are observables, while the other magnitudes are given. The time variations of the solar coordinates are usually expressed by the proper motions $\mu_{\alpha,\odot} = d\alpha_\odot/dt$ and $\mu_{\delta,\odot} = d\delta_\odot/dt$, giving

$$\omega = \sqrt{\mu_{\alpha,\odot}^2 \cos^2\delta_\odot + \mu_{\delta,\odot}^2}. \tag{7}$$

Therefore, a simple method to determine ω is to measure the time $\Delta t_\odot^{\mathrm{t}}$ elapsed between two transits separated by a few days (N_{days}), and the corresponding difference $\Delta z_\odot^{\mathrm{t}}$ of the zenith distances of the Sun. In this case, Eq. (6) transforms into

$$\mu_{\alpha,\odot} \approx \frac{\Delta\alpha_\odot}{\Delta t_\odot^{\mathrm{t}}} = \frac{\Omega_\oplus \Delta t_\odot^{\mathrm{t}} - 2N_{\mathrm{days}}\pi}{\Delta t_\odot^{\mathrm{t}}}, \tag{8}$$

where the term $-2N_{\mathrm{days}}\,\pi$ accounts for the whole turns completed by Earth between the two transits. On the other hand, Eq. (5) reads

$$\mu_{\delta,\odot} \approx \frac{\Delta\delta_\odot}{\Delta t_\odot^{\mathrm{t}}} = \pm\frac{\Delta z_\odot^{\mathrm{t}}}{\Delta t_\odot^{\mathrm{t}}}. \tag{9}$$

Equations (8) and (9) depend only on observables and can be used together with Eq. (7) to determine the angular velocity ω of Earth.

Moreover, from the equatorial coordinates of the Sun [Eqs. (5) and (6)] and the proper motions [Eqs. (8) and (9)], the unit vector in the direction of Earth angular momentum can also be computed

$$\hat{L}_\oplus = \hat{r}_\odot \times \hat{v}_{\mathrm{t},\odot} = \omega^{-1}(\mu_{\alpha,\odot}\cos\delta_\odot \hat{\delta}_\odot - \mu_{\delta,\odot}\hat{\alpha}_\odot). \tag{10}$$

Here, $\hat{\alpha}_\odot$ and $\hat{\delta}_\odot$ are the spherical unit vectors of the equatorial reference frame at the position of the Sun, and hence depend on the latter. To verify its constancy, $\hat{L}_\oplus$ must be written in terms of the fixed Cartesian unit vectors $(\hat{X}, \hat{Y}, \hat{Z})$ defined above. The relationship between the two sets of unit vectors is

$$\hat{\alpha}_\odot = -\sin\alpha_\odot \hat{X} + \cos\alpha_\odot \hat{Y}, \tag{11}$$

and

$$\hat{\delta}_\odot = -\sin\delta_\odot \cos\alpha_\odot \hat{X} - \sin\delta_\odot \sin\alpha_\odot \hat{Y} + \cos\delta_\odot \hat{Z}. \tag{12}$$

The above discussion shows that a set of simultaneous observations of the position, apparent radius, and proper motion of the solar disk allows the computation of the orbital angular momentum of Earth. Repeating the observations several times during an interval comparable to Earth orbital period (i.e., several months), the conservation of angular momentum can be demonstrated. It is important to note that the minimum and maximum distances between Earth and the Sun are reached in early January and July, respectively. Therefore, the observations should not be clustered around these dates, as the changes in the distance are then small.

It is interesting to note the relation between the aforementioned observables and two constructions used in astronomy to visualize the nonuniformity of the motion of the Sun during the year. The first one is the *equation of time* (EoT),[18] defined as the difference in right ascension between the true and mean Sun, the latter being a fictitious object moving uniformly along the equator so that its transits are always separated by 24 h. Therefore, the rate of change of the EoT traces the nonuniform component of the motion of the Sun, projected onto the equator. Hence, a determination of the EoT[20] would allow the computation of $\Delta\alpha_\odot$, after adding the mean solar motion. Note, however, that the latter amounts to $\sim$4 min per day, typically an order of magnitude larger than the EoT variations. The second construction is the *solar analemma*, a figure-eight-shaped graph obtained by plotting the declination of the Sun against the EoT along the year or, in other cases, the elevation of the Sun at mean local noon against its azimuth.[17] In the EoT-declination version, the variation of the east-west component of the solar analemma from one observation to the next is $\Delta\alpha_\odot$ minus the mean Sun motion, whereas the change in the north-south component is directly $\Delta\delta_\odot$. Therefore, measuring the components of the velocity of the Sun along the analemma and correcting for the mean Sun motion and the $\cos\delta_\odot$ factor of Eq. (7) would be a direct and elegant measurement of ω. However, for reasons that will be explained in Sec. III, the precision required for the present demonstration cannot be achieved by taking measurements directly from the analemma.

III. EXPERIMENTAL SETUP

The goal of the present experiment is to accurately measure the position, apparent radius, and proper motion of the Sun at different times. In order to see a change in these magnitudes, the measurements must span a period of several months, during which Earth moves from near its perihelion to near its aphelion. Despite this fact, the experiment requires relatively little time, because one or two observations per month are enough to demonstrate the constancy of angular

momentum. We performed the experiment in Buenos Aires, Argentina, from July 3 to December 24, 2014. We recall that the time of aphelion was July 4, 2014, while that of perihelion was January 4, 2015.[21]

The critical experimental requirement is a precision of $\sim$0.3% in the apparent radius $\phi_\odot$ of the Sun. To achieve this precision, we chose a small telescope equipped with a full-aperture solar filter and a six-megapixel digital camera to image the Sun. We performed the experiment at the Galileo Galilei Observatory of the Cristoforo Colombo Italian School of Buenos Aires, which is equipped with a 203-mm-aperture, *f*/6.3-focal-ratio, Meade LX200 Schmidt-Cassegrain telescope with an alt-azimuth mount. A Thousand Oaks Type 2+, full-aperture solar filter with a transmission of 10^{-5} was attached to the telescope. A Canon EOS Digital Rebel (Canon EOS 300D) reflex camera was used to take the images. This camera has a 22.7×15.1 mm sensor with 2048×3072 pixels of 7.4 μm in size. The image of the Sun in the focal plane of the telescope is $\sim$12 mm, or about 1800 pixels, which allows us to get almost the largest resolution possible with this camera. The nominal precision for the measurement of the apparent radius is then of the order of 0.1%, corresponding to a one-pixel uncertainty.

Before the first observation, we focused the camera on the Sun and took a set of test images to determine the best exposure time. A value of 1/3200 s at ISO 800 was chosen and was used in every observation, because the luminosity of the Sun does not change, the telescope aperture, focal length, and filter transmission are fixed, and the changes in the atmospheric extinction are small. We measured the size of the solar disk on the images directly in pixels and used the scale of the images ($\xi = 1.087$ arc sec pix^{-1}) to determine $\phi_\odot$. Although the scale depends on the focal length of the telescope and the pixel size,[22] the effective focal length of the Meade LX200 telescope is different from its nominal value, and depends on the distance between the camera and the rear end of the telescope. Therefore, we measured the scale of our particular telescope-plus-camera configuration (except for the solar filter) by taking an image of a stellar field and comparing the positions of a set of stars with known coordinates, taken from the Smithsonian Astrophysical Observatory Star Catalog.[23] Given the value obtained and the resolution limit imposed by atmospheric seeing (of the order of a few arcsec), the experimental configuration provides a reasonable coupling between atmospheric and detector resolution. We checked that there were no temperature variations of the scale for the ambient temperature range in which the experiment was performed (17 °C–29 °C).

The measurement of the solar coordinates and proper motion can be performed following the procedure described in Sec. II. The time and zenith distance of the transit of the Sun can be measured at two epochs separated by a few days, and Eqs. (7)–(9) used to determine the solar coordinates, their variation, and ω. However, for the determination of $\Delta z^{\mathrm{t}}_\odot$, the direct use of this procedure is prone to cancelation errors, because $\Delta z^{\mathrm{t}}_\odot = z^{\mathrm{t}}_{\odot,2} - z^{\mathrm{t}}_{\odot,1}$ is the difference of two much greater quantities.[24] From Eq. (5), with a latitude $\varphi \approx -35°$, $z^{\mathrm{t}}_\odot \gtrsim 12°$, while $\Delta z^{\mathrm{t}}_\odot$ is $\sim$100 times smaller. Therefore, to determine $\Delta z^{\mathrm{t}}_\odot$ with a precision of 1% would require an extremely high precision of 0.01% in the determination of $z^{\mathrm{t}}_\odot$, which we cannot achieve with our equipment. To avoid this problem, we aimed at measuring the difference $\Delta z^{\mathrm{t}}_\odot$ directly, by imaging the path of the Sun in the sky near its transit at two epochs separated by a few days;[25] the vertical difference between the two paths is $\Delta z^{\mathrm{t}}_\odot$. To achieve this, the first day of each observation we pointed the telescope to the meridian with a reasonable precision (our telescope allows us to do it within 0.125°), and fixed its azimuth. We oriented the camera in such a way that the long size of the chip is horizontal, to observe the largest possible path of the Sun in the sky.[26] When the Sun entered the field of view of the camera, we roughly centered its image vertically and fixed the telescope at this altitude. We took a series of snapshots with the telescope fixed (i.e., disabling the tracking of celestial bodies) as the solar disk moves through the field of view of the camera. The second day we took a second, similar series of snapshots, keeping the telescope fixed at the position in which we left it the first day. The camera acts here as a reference frame fixed to Earth, and the trail described by the solar disk in the snapshots correspond to its path near each transit. The vertical difference between the two trails is directly $\Delta z^{\mathrm{t}}_\odot$, and the nominal precision of the measurement is equal to the resolution of the camera (1 pix $\approx$ 1 arc sec).

Note that it is not crucial that the camera is oriented exactly in the horizontal direction. Any orientation error can be corrected for using the fact that the solar path during transit is horizontal. Moreover, the procedure is also robust against small errors in the pointing azimuth of the telescope. A small systematic error is committed in the determination of $z^{\mathrm{t}}_\odot$ due to the curvature of the solar path in the sky. Its magnitude can be estimated using the formulae for transformation between the horizontal and equatorial coordinate systems[18] and amounts to $\lesssim$5 arc sec for our 0.125° pointing accuracy. As the curvature is similar for both days in each observation, the systematic error in Δz is much less than this value, and can be neglected. The leveling of the base of the telescope, although performed carefully, is not an issue for this measurement. It changes the individual values of $z^{\mathrm{t}}_{\odot,j}$ (here, j indicates the observation day) by the same amount, hence it cancels in the difference $\Delta z^{\mathrm{t}}_\odot$.

The procedure described above also allows measurement of the variation in transit times $\Delta t^{\mathrm{t}}_\odot$. The camera records the time at which each snapshot was taken. We used these values to determine the time $t^{\mathrm{t}}_{\odot,j}$ at which the center of the solar disk crossed the central pixel column of the chip each day. The difference of these times is $\Delta t^{\mathrm{t}}_\odot = t^{\mathrm{t}}_{\odot,2} - t^{\mathrm{t}}_{\odot,1}$. Once again, this difference is not affected by small pointing errors, as the angular velocity of the Sun is nearly constant between the two observations, and its path near transit is horizontal. The systematic uncertainty in the transit times due to pointing errors can be estimated in the same way as the systematic uncertainty in $\Delta z^{\mathrm{t}}_\odot$. For our pointing precision, it amounts to less than 0.4 s in $\Delta t^{\mathrm{t}}_\odot$, or less than 6 arc sec in $\Delta\alpha_\odot$. The leveling accuracy has no effect on the measurement of $\Delta t^{\mathrm{t}}_\odot$, and the precision of the internal camera clock is not an issue, as the worst quartz clocks are accurate to 0.5 s per day.[27] As a by-product, each value of $t^{\mathrm{t}}_\odot$ can be used, together with the time of transit of the vernal equinox that day (taken from the Data Services of the United States Naval Observatory[21]) and Eq. (6) to determine the right ascension of the Sun $\alpha_\odot$. Its declination can be determined from Eq. (5) and the value of the fixed altitude of the telescope (the complement of the zenith distance), which can be read from its setting circles with a precision of 0.125°.

The raw outcome of the experiment is therefore a set of observations, each one comprising several images to measure the apparent radius of the solar disk, and two series of

snapshots describing the path of the Sun in the sky near transit, at epochs separated by a few days. Each snapshot records the time at which it was taken. The altitude of the telescope at each observation and the number of days elapsed between the two series of snapshots (in our case always one) is also recorded. In Sec. IV, we will describe the analysis of the data of each set, and the computation of the angular momentum of Earth.

IV. DATA ANALYSIS AND RESULTS

As a first step in the analysis of the data, we determined the apparent radius $\phi_\odot$ of the solar disk during each observation. Due to atmospheric refraction and extinction, and to the conditions in the photosphere, the solar limb is not sharp. A radial intensity profile (Fig. 2) shows instead a smooth decline of the brightness towards the limb. The best definition of the position of the limb is therefore the location of the maximum absolute value of the slope of the intensity (vertical dashed line in Fig. 2).[28,29] Hereafter, to express positions in the images, we will use a reference system with its origin at the center of the chip (i.e., at pixel [1536, 1024]) and the x (y) axis along rows (columns). To find the points (x, y) belonging to the limb, we took $N = 500$ columns at positions x_i near the center of the solar disk, computed the differences of the intensity between adjacent pixels along each of them, and determined the positions $y_{i,+}$ and $y_{i,-}$ where the maximum positive and negative intensity change occurs, respectively. To avoid spurious, abrupt variations due to noise, we smoothed the intensity profiles along the columns using a three-pixel moving-average filter before computing the differences. As $y_{i,+/-}$ mark the position of the limb for a given column, $y_{c,i} = (y_{i,+} + y_{i,-})/2$ gives an estimation of the row of the center of the solar disk. The uncertainty of this estimation is of the order of $\sim$5 pix. The mean of $y_{c,i}$ over all columns, $y_c = N^{-1} \sum_i y_{c,i}$, gives the y coordinate of the center of the solar disk, with subpixel precision. Applying the same procedure to N rows, we obtain the x coordinate of the center, x_c.

Given the $4N$ points of the limb determined with the previous procedure, we fitted a circle to them by applying the least-squares method to the equation

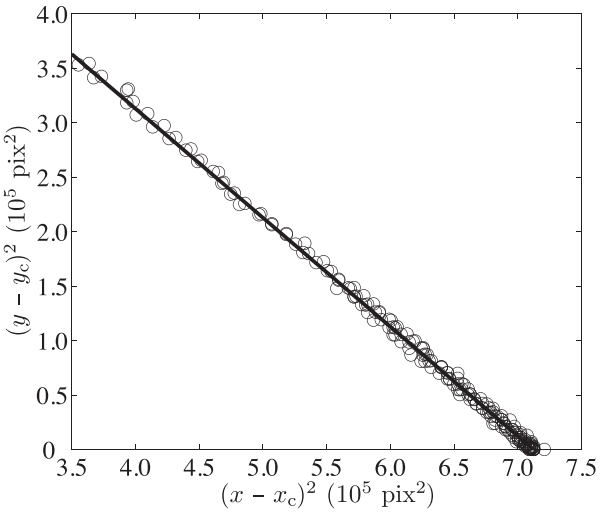

Fig. 3. Determination of the solar disk radius. For each limb point (x, y), $(y - y_c)^2$ is plotted as a function of $(x - x_c)^2$ (circles). The intercept of the linear correlation (solid line) between these quantities is R^2_{limb}. For the sake of clarity, only 10% of the 2000 data points used in the fit are plotted.

$$(y - y_c)^2 + (x - x_c)^2 = R^2_{\text{limb}} \tag{13}$$

to determine the limb radius R_{limb} (Fig. 3). The apparent radius of the Sun was then computed as $\phi_\odot = \xi R_{\text{limb}}$, and its distance was computed from Eq. (3). The advantages of this technique are its simplicity and precision. As the solar limb is defined by 2000 points, the effect of random distortions of the image (such as those produced by atmospheric seeing) averages out. This reduces the five-pixel uncertainty of each limb position to a 0.3-pixel statistical error in the estimation of R_{limb}. The main source of systematic error is the flattening of the solar disk due to differential atmospheric refraction. The transit occurs at altitudes higher than 30° at our latitude, leading to a shortening of the vertical radius of the Sun by less than 2 arc sec ($\sim$2 pix).[18] To be conservative, we took this value as the total error of our measurement.

As this is the crucial measurement of the experiment, it is worthwhile to compare its results to those obtained from precise ephemeris of Earth's orbit;[21] Fig. 4 shows this

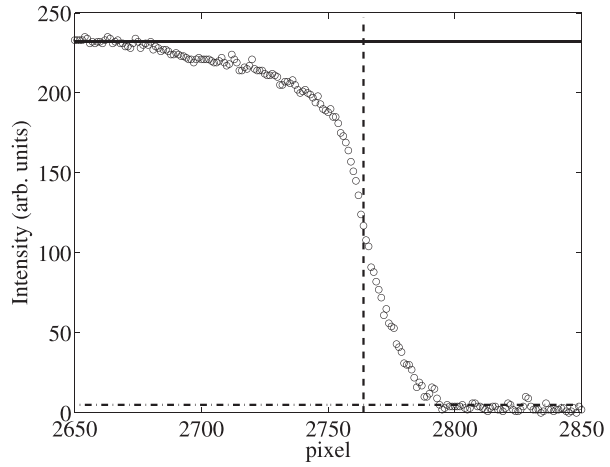

Fig. 2. Radial intensity profile of the solar disk. A smooth decline from the brightness level of the solar disk (solid line) to the sky level (dotted-dashed line) is seen. The maximum slope of the profile marks the position of the solar limb (dashed line).

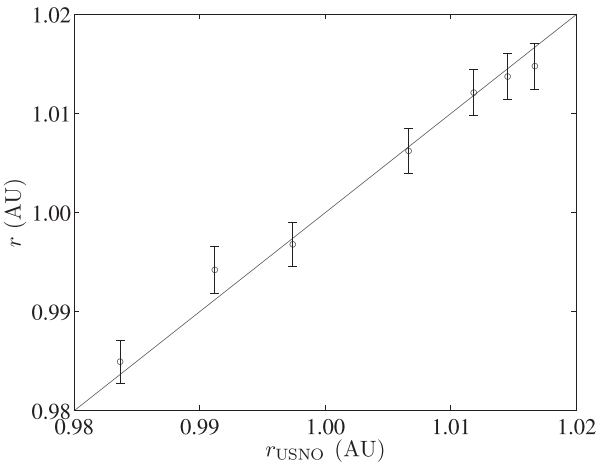

Fig. 4. Comparison between our estimation of the distance to the Sun (r) and precise ephemeris obtained from the U.S. Naval Observatory (r_{USNO}) for the dates of our observations. The data are consistent with the identity (solid line) to within experimental errors, showing the correctness of our method.

comparison. A clear correlation is seen, with the data scattered around the identity (solid line in the figure), indicating that our method is both precise and accurate. The scatter is of the order of the size of the error bars, demonstrating that the uncertainties are estimated correctly. In brief, Fig. 4 shows that our method provides an adequate estimation of the distance of the Sun.

To measure the angular velocity of the Sun for each observation, we used the series of snapshots taken to determine its path in the sky between two consecutive days. For each snapshot, we determined by eye the circle of radius $R_{\rm limb}$ passing as close as possible to the solar limb position. Here, $R_{\rm limb}$ is the limb radius obtained for the same observation using the procedure described above. We used for this purpose the Smithsonian Astrophysical Observatory SAOImage DS9 software,[30] which allows us to draw a circle of a given radius on any image and determine the position of its center (x_c, y_c). We note that in this case the exact definition of the solar limb is irrelevant, because we do not want to measure its radius, and the fitting is guided by the symmetry of the solar disk rather than by the exact location of the limb points. Although this procedure is less precise (the uncertainty in the measured position is $\sim$5 pix), it is good enough for the purpose of computing the solar proper motion. In any case, the previous, more precise method for determining the position of the center of the Sun cannot be applied, because most images do not show the complete solar disk.

The positions (x_c, y_c) trace the paths of the Sun in the sky near transit for both days. Figure 5 (left panel) presents a set of snapshots showing the motion of the Sun through the field of view of the camera the first day of one observation. It can be seen that the path is straight, indicating the direction parallel to the horizon. This figure also shows that the orientation of the camera is not perfect. To correct this misalignment, we plotted the positions (x_c, y_c) for each day (right panel of Fig. 5) and fitted a straight line to them by least squares. The average of the two slopes determines the rotation angle ε between the x axis of the images and the horizontal direction.

Using the rotation angle ε, we transformed the positions (x_c, y_c) to a reference frame with axes (x', y') rotated counterclockwise by ε with respect to the (x, y) axes. This makes the paths run along the x'-axis of the new frame. Because the y'-axis is perpendicular to the horizon by construction, the average $y'_{p,j}$ of the y'_c values for each day j gives the altitude of the path of the Sun for that day, up to the multiplicative scale factor and an additive constant. This constant is the pointing altitude of the telescope, and although we have measured it, we do not use it for this computation because its relative error is too large. Instead, we compute the difference $\Delta y'_p = y'_{p,2} - y'_{p,1}$, in which the additive constant cancels out. This difference is related to the variation in the solar zenith distance at transit between both days, by $\Delta z^t_\odot = -\xi \Delta y'_p$.

To determine the variation of the solar right ascension, we plot for both days the x'-coordinate of the solar disk against the time at which each snapshot was taken (Fig. 6). It can be seen that the relationship between these magnitudes is linear, due to the constancy of the solar angular velocity during the three minutes that the series of snapshots lasts. A least-squares fit of a linear function gives the parameters of this relationship, and hence the time $t^t_{\odot,j}$ at which the Sun crossed each day the center of the image ($x' = 0$, which is the location of the meridian to within the experimental uncertainty). The time between the two transits is then $\Delta t^t_\odot = t^t_{\odot,2} - t^t_{\odot,1} + 24^h$, as each $t^t_{\odot,j}$ is measured from the previous midnight (mean solar time). The nominal uncertainty of the determination of $\Delta t^t_\odot$ by this method is of the order of 0.1 s. However, because digital clocks could introduce errors $\lesssim$0.5 s per day,[27] we conservatively take this figure as the uncertainty of $\Delta t^t_\odot$.

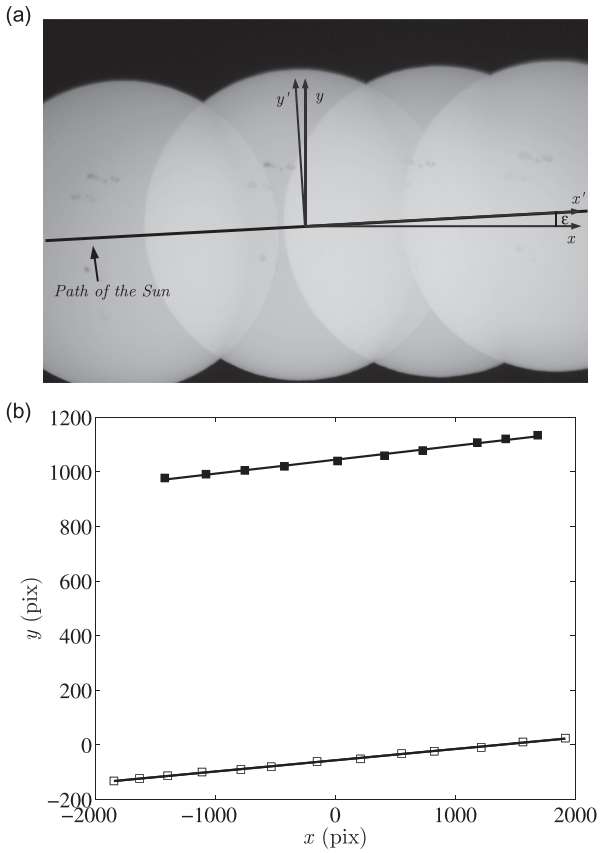

Fig. 5. Upper panel: Composite image showing the motion of the Sun near its transit. Four frames taken during an interval of 3 min with the telescope fixed and pointing to the local meridian were combined. The solid line shows the path of the center of the Sun through the field of view. Because this path is horizontal, it helps us in transforming the image reference frame (x, y) to a new one with its axes (x', y') aligned to the horizon. Lower panel: Positions of the Sun near its transit during the first (open squares) and second (filled squares) days of an observation. The average slope of the fits (solid lines) gives the misalignment ε of the camera. The size of the squares is the nominal measurement error of $\pm$5 pix.

We used the measured value of $\Delta t^t_\odot$ in Eq. (8) to determine $\mu_{\alpha,\odot}$ and, together with $\Delta z^t_\odot$, in Eq. (9) to obtain $\mu_{\delta,\odot}$. Using the value of the fixed altitude of the telescope, we computed the solar zenith distance $z_\odot$ and declination $\delta_\odot$ [Eq. (5)] at the first transit. From these quantities, we determined the angular velocity of the Sun ω [Eq. (7)] and, using the measurement of $r_\odot$ described previously, the magnitude of the angular momentum of Earth $L_\oplus$. The time of the first transit, together with that of the vernal equinox ($\alpha_\star = 0$, tabulated[21]) and Eq. (6), allowed us to determine the right ascension $\alpha_\odot$. In this way, we determined the position of the Sun at the first transit. Using the computed solar position and proper motion, we obtained the direction of the angular momentum of Earth $\hat{L}_\oplus$ [Eq. (10)].

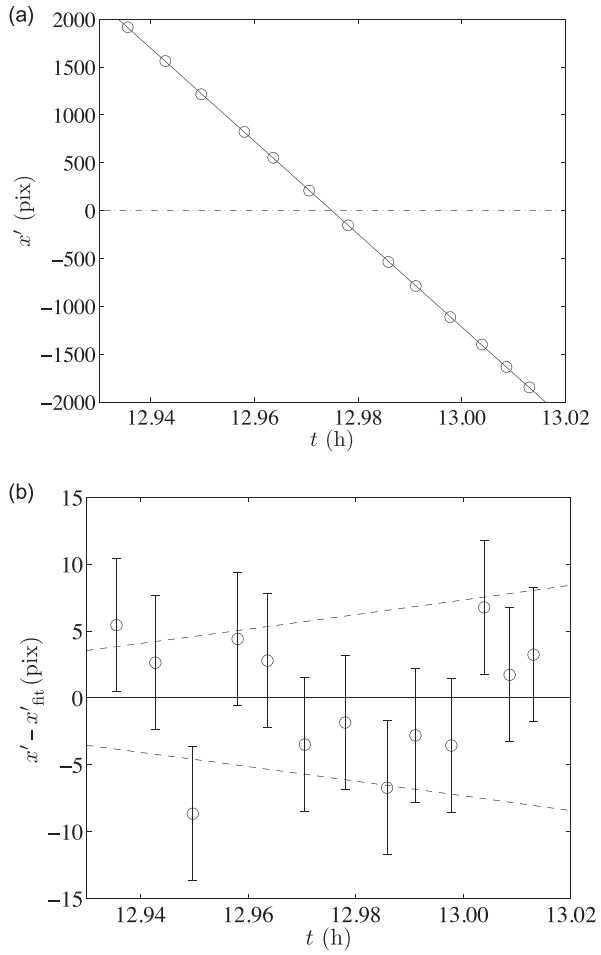

Fig. 6. Determination of the solar transit time. The upper panel shows the position x' of the solar disk center as a function of time t. Open circles represent the data, while the solid line is a linear fit. The dot-dashed line marks the position of the meridian, hence its intersection with the fit is the transit time. The lower panel shows the residuals of the fit. The uncertainties of the data are plotted as well as the 68% confidence region of the fit (dashed lines) to show its quality.

Figure 7 shows the relation between the distance to the Sun $r_\odot$ and its angular velocity ω. A clear trend can be seen, in the sense that the angular velocity decreases with increasing distance. Moreover, this trend is consistent with a power-law relation, as required by Eq. (2). A least-squares fit gives an exponent of -2.31 ± 0.33 for this relation, consistent with the value -2 expected from the conservation of angular momentum within the 68% confidence level. The fit was performed using the effective variance method, as the relative uncertainties in both axes are of the same order of magnitude. We note that despite the high precision of the data (below 1%), that of the slope is only ∼15%. The precision is low because the variations of the magnitudes being measured are much smaller than their values. On the one hand, this highlights the importance of our initial analysis, in which we adopted a goal precision of 0.3% for our measurements after examining carefully the magnitude of the effect to be measured. Note that the whole experimental setup is based on this analysis. On the other hand, this result shows that a higher precision in the slope (say, of the order of 1%) is unreachable with commercial, low-cost equipment. To show explicitly the conservation of angular momentum, we computed the magnitude of $L_\oplus/M_\oplus$ and plotted it against the observation date (Fig. 8). The constancy of the magnitude of the angular momentum of Earth, to within the 2% precision of our data, is clear in this figure. The mean value is $L_\oplus/M_\oplus = 6.28 \pm 0.04$ AU^2 yr^{-1}.

The conservation of the direction of $L_\oplus$ is demonstrated in Fig. 9. The three Cartesian components of the unit vector $\hat{L}_\oplus$, computed from our data, are shown. The X-component is consistent with a null value, as expected because the equatorial reference frame has the X-axis along the intersection of the ecliptic with the celestial equator, hence in the plane of motion of Earth. The other two are constant to within 3%. The inclination of the orbit of Earth (the ecliptic) with respect to its equator can be obtained from these components (e.g., $\tan\epsilon = L_{\oplus,Y}/L_{\oplus,Z}$). From our data, $\epsilon = 23.35 \pm 0.05°$, in good agreement with the mean obliquity for the year 2014, $\epsilon = 23.44$.[21]

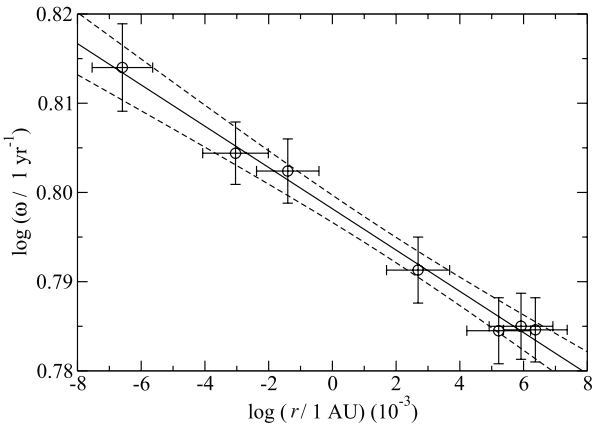

Fig. 7. Log-log plot of the angular velocity of Earth as a function of the distance to the Sun. A clear correlation is seen, the best-fit power law (solid line) having a slope of -2.31 ± 0.33, consistent with the value of -2 expected from the conservation of angular momentum. Dashed lines show the 68% confidence region.

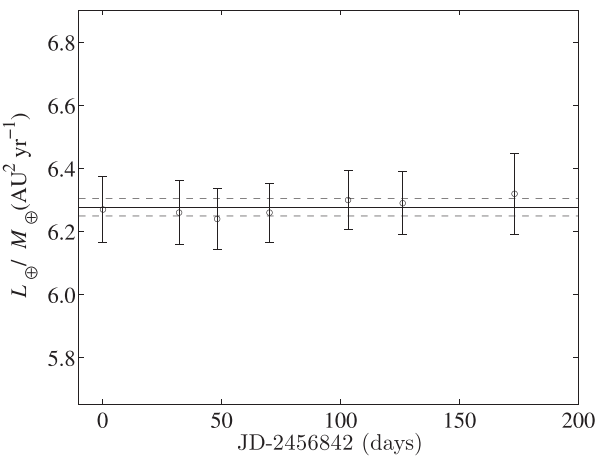

Fig. 8. Magnitude of the specific angular momentum of Earth as a function of the observation date. The conservation of $L_\oplus/M_\oplus$ to within the experimental uncertainty of 2% is evident. The solid line shows the mean values of $L_\oplus/M_\oplus$, while the dashed lines show the standard deviation of the data. Dates are given as Julian Date minus the date of the first observation.

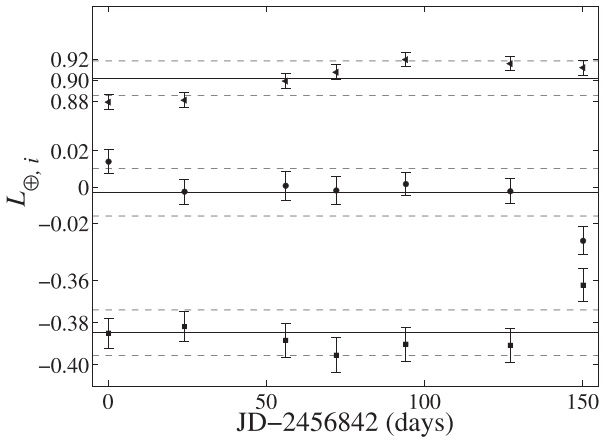

Fig. 9. Direction of the specific angular momentum of Earth as a function of the observation date. The Cartesian components of $\hat{L}_{\oplus}$ are plotted as circles ($L_{\oplus,X}$), squares ($L_{\oplus,Y}$), and triangles ($L_{\oplus,Z}$). Solid lines are the corresponding mean values, while dashed lines represent three times the standard deviation of the data. The component $L_{\oplus,X}$ is null as expected, because the X-axis lies in the plane of the ecliptic. The other two components are constant within experimental errors and give the obliquity of the ecliptic ($\epsilon = 23.35 \pm 0.05°$). Dates are given as Julian Date (JD) minus the date of the first observation (JD 2456842 = 2014 July 3).

V. CONCLUSIONS

The experiment described here allows one to verify the conservation of both the direction and the magnitude of Earth's angular momentum vector to within a few percent. We believe that this experiment is unique in the sense that it provides quantitative evidence for one the central principles of physics, and also for the central nature of one of the fundamental interactions. Because Earth-Sun system is simple in terms of the dynamical interaction between its components, the results can be easily and clearly interpreted by students, providing them with direct insight into the physics involved.

Two crucial features of the experiment are responsible for its success. The first is the high precision (below 1%) achievable for each individual photographic measurement. This level of precision is needed to obtain useful data that correctly trace the small variation of the observables (the Sun's apparent size and angular velocity), which amounts to a few percent. A careful instrumental setup and an extensive data analysis are then mandatory, as well as a thorough investigation of the error sources, both statistical and systematic. The second crucial feature is the method of measuring the variation of the position of the Sun, using directly the difference of observables (time and altitude of transit) on two consecutive days. A separate measurement of the position each day would suffer from cancellation errors, and would prevent the required precision from being reached. The precision of the method allows the separation of the angular velocity component due to the orbital motion of Earth from the much larger one due to the rotation of our planet.

Due to the aforementioned features, we believe that this experiment poses an interesting challenge to undergraduate students, allowing them to improve their knowledge of fundamental mechanics while training themselves in astronomical observation and data analysis techniques.

ACKNOWLEDGMENTS

The authors are indebted to Lic. J. Bertúa and the authorities of the Scuola Italiana Cristoforo Colombo of Buenos Aires, Argentina, for the strong support given to this project. The authors are also grateful to the Department of Natural Sciences of Cristoforo Colombo, for lending the digital camera used in this work. Finally, the authors would like to acknowledge the anonymous referees for their comments, which helped to greatly improve our manuscript.

[a]Electronic mail: pellizza@iar.unlp.edu.ar
[b]Consejo Nacional de Investigaciones Científicas y Técnicas, Argentina.

[1]H. Goldstein, *Classical Mechanics*, 2nd ed. (Addison Wesley, New York, 1980).
[2]J. D. Jackson, *Classical Electrodynamics*, 2nd ed. (Wiley, New York, 1975).
[3]C. Cohen-Tannoudji, L. Diu, and F. Lalöe, *Quantum Mechanics* (Wiley-Interscience, New York, 1977).
[4]W. C. Connolly and R. C. Connolly, "Angular momentum demonstration," Am. J. Phys. **41**, 131–132 (1973).
[5]H. Klostergaard, "Conservation of angular momentum—A demonstration," Am. J. Phys. **44**, 21 (1976).
[6]S. Datta, "Demonstrations of angular momentum," Am. J. Phys. **46**, 1190–1192 (1978).
[7]F. Herrmann and G. Bruno Schmid, "Demonstration of angular momentum coupling between rotating systems," Am. J. Phys. **53**, 735–737 (1985).
[8]S. Y. Mak and K. Y. Wong, "A qualitative demonstration of the conservation of angular momentum in a system of two noncoaxial rotating disks," Am. J. Phys. **57**, 951–952 (1989).
[9]M. Gardner, "The twirled ring," Phys. Teach. **40**, 51 (2002).
[10]D. L. Mott, "Demonstrating conservation of angular momentum," Phys. Teach. **43**, 552 (2005).
[11]T. M. Kalotas and A. R. Lee, "A simple device to illustrate angular momentum conservation and instability," Am. J. Phys. **58**, 80–81 (1990).
[12]R. E. Berg and R. E. Anders, "Angular momentum conservation demonstration," Phys. Teach. **27**, 561–562 (1989).
[13]R. Carr, H. Cohen, and T. Ragsdale, "Demonstrating angular momentum conservation," Phys. Teach. **37**, 169–171 (1999).
[14]K. Altshuler and P. Pollock, "Inexpensive rotating-arm device for angular-motion labs," Phys. Teach. **36**, 424–425 (1998).
[15]A. Saitoh, "Law of conservation of momentum apparatus," Phys. Teach. **44**, 546–548 (2006).
[16]J. C. Williamson, R. O. Torres-Isea, and C. A. Kletzing, "Analyzing linear and angular momentum conservation in digital videos of puck collisions," Am. J. Phys. **68**, 841–847 (2000).
[17]M. Zeilik and E. van Panhuys Smith, *Introductory Astronomy and Astrophysics* (Saunders College Publishing, New York, 1987).
[18]J. Meeus, *Astronomical Algorithms* (Willmann-Bell, Richmond, 1991).
[19]We will express both equatorial coordinates in radians to simplify the equations.
[20]T. Lahaye, "Measuring the eccentricity of Earth's orbit with a nail and a piece of plywood," Eur. J. Phys. **33**, 1167–1178 (2012).
[21]United States Naval Observatory data services, <http://aa.usno.navy.mil/data/>.
[22]E. Hecht, *Optics*, 2nd ed. (Addison-Wesley, New York, 1987).
[23]SAO Star catalog J2000, <http://vizier.cfa.harvard.edu/viz-bin/VizieR?-source=I/131A>.
[24]The subscripts 1 and 2 refer here to the first and second day of the observation, respectively.
[25]Ideally, the experiment should be performed on two consecutive dates. However, if this is not possible (for example, due to weather conditions), the observer must ensure that the detector is large enough in the vertical direction to accommodate the motion of the Sun in declination. In our experiment, all the observations were made on consecutive dates.
[26]We disregard here the small variation in the solar coordinates during the few minutes it takes to go across the field of view of the camera.

[27]M. A. Lombardi, "The evolution of time measurement, Part 2: Quartz clocks," IEEE Instrum. Meas. Mag. **14**, 41–48 (2011).
[28]L. Gyori, "Determination of atmospheric refraction from the distortion of the Sun's disc," Astron. Astrophys. **278**, 659–664 (1993).
[29]L. J. Pellizza, M. G. Mayochi, and L. Ciocci Brazzano, "An experiment to measure the instantaneous distance to the Moon," Am. J. Phys. **82**, 311–316 (2014).
[30]SAOImage DS9 software, <http://ds9.si.edu/site/Home.html>.

Three-arm Spectrometer

The third arm (the one in the front right of the picture) uses the light from a gas flame to project the image of a transparent glass scale into the telescope by reflecting it off the near face of the prism. In use, the light from a standard element is also sent through the collimator, so that the user sees one spectrum on top of the other and both against the image of the scale. The lines of the unknown are then compared with the lines of the known. This instrument is listed at $35.00 in the 1888 Queen catalogue. Note that the eyepiece on the telescope and the objective of the collimator are missing. It is rare to find a complete spectrometer, as these lenses make handy magnifiers. This example is in the Greenslade Collection. (Notes and picture by Thomas B. Greenslade, Jr., Kenyon College)